Artikel 18

by Rahayu Aster

Submission date: 30-Mar-2023 03:33AM (UTC+0700)
Submission ID: 2050271624
File name: s_Residue_with_Silica-_alumina_Catalyst_Through_5-Lump_Model.pdf (620.92K)
Word count: 6501
Character count: 33469

Reaction kinetics of Components of Ex-Situ Slow Pyrolysis of *Spirulina Platensis* Residue with Silica-alumina Catalyst Through 5-Lump Model

Siti Jamilatun*‡, Dhias Cahya Hakika*, Nuraini*, Joko Pitoyo*, Martomo Setyawan*, Arief Budiman**, Aster Rahayu*

*Department of Chemical Engineering, Faculty of Industrial Technology, Universitas Ahmad Dahlan, Jl. Jend. Ahmad Yani Banguntapan Bantul, Yogyakarta, Indonesia 55166

**Department of Chemical Engineering, Faculty of Engineering, Universitas Gadjah Mada, Jl. Grafika No. 2 Kampus UGM, Yogyakarta, Indonesia 55281

(sitijamilatun@che.uad.ac.id, dhias.hakika@che.uad.ac.id, nuraini1800020131@webmail.uad.ac.id, martomo@che.uad.ac.id, abudiman@ugm.ac.id, aster.rahayu@che.uad.ac.id)

‡Corresponding Author; Siti Jamilatun, Department of Chemical Engineering, Faculty of Industrial Technology, Universitas Ahmad Dahlan, Indonesia 55166, Tel: +6281329157053, sitijamilatun@che.uad.ac.id

Received: xx.xx.xxxx Accepted:xx.xx.xxxx

Abstract- Pyrolysis *Spirulina platensis* residue (SPR) processing/produces tar, char, and gas products. Tar upgrading with a catalyst is carried out to reduce the oxygenate content in the tar. The reaction kinetics of oxygenate compounds in tar to form aliphatic, aromatic, oxygenate, and coke and gas compounds must be calculated. The calculation determines the reaction rate constant (k) and activation energy (E) value. This paper discusses the catalytic kinetic components of ex-situ slow pyrolysis of *Spirulina platensis* residue with silica-alumina via a 5-lump model. Values of k and E can predict the predominance of product compound formation tendencies and are required for industrial design. A fixed-bed reactor with a silica-alumina catalyst operates with a temperature range of 300–600°C, the thickness of the catalyst in the reactor R2 is 0–4.5 cm, and the heating rate is 5–35°C/min. The reactor consists of two (2) vertical cylinders, reactor R1 contains the SPR, and reactor R2 is filled with the catalyst. Based on experimental data, the decomposition of oxygenating products into aliphatic products is more dominant than the decomposition of aliphatic and aromatic compounds into other products. The dominance of aliphatic formation is indicated by the lowest activation energy value (0.07 kJ/mol) occurring in the k_6 reaction (11.779-11.835 $sec.^{-1}$), i.e., the oxygenate product becomes aliphatic. The lowest E value indicates oxygenate compounds are more easily decomposed than aromatic and aliphatic compounds. The product oxygenates, aliphatic, aromatic, coke, and gas compounds increased with increasing catalyst thickness; on the other hand, the pyrolysis feed oxygenate compound decreased sharply.

Keywords *Spirulina platensis* residue; reaction rate constant; activation energy; reaction kinetics; 5-lump model.

1. Introduction

The soaring price of fuels from fossil sources and the depletion of energy reserves have searched for an essential alternative and sustainable energy source. Biomass has received significant attention worldwide as a renewable carbon source and is used to generate power, electricity, fuels, and other valuable by-products [1]. The topic of great interest to researchers is the supply of renewable fuels and chemicals from biomass pyrolysis. Thermochemical, biochemical, chemical, and physical conversion have been widely developed for processing biomass [2], [3]. One widely grown process is thermochemistry, including liquefaction, pyrolysis, gasification, and combustion [4], [5]. Some advantages of pyrolysis compared to other technologies are the form of a pyrolysis unit with a simple reactor arrangement, short reaction time, lower energy requirements for product separation, and adaptability to various types of biomass [1], [6]. Pyrolysis gas, charcoal, and tar products can be used for multiple purposes. Char can be used as an adsorbent, while tar and gas have a large enough energy for fuel [7], [8]. One attractive biomass to develop is

the microalgae Spirulina platensis, rich in protein, carbohydrates, and lipids. Spirulina platensis residue (SPR) is the waste from processing the microalgae Spirulina platensis after the lipids are extracted. Its extractions are still rich in carbohydrates and proteins, then the opportunity for biomass as a world energy source needs to be increased [7], [9], [10].

So far, many studies have been carried out to process microalgae with or without a catalyst using pyrolysis technology [11]. Tar produced from uncatalyzed pyrolysis still contains high oxygenate compounds [12]. Reducing the content of oxygenated compounds in tar can use a pyrolysis catalyst [10]. Tar production on an industrial scale still needs to be developed, and the feasibility of the process needs to be evaluated, especially regarding the reactor design. Data on kinetics and decomposition characteristics are indispensable in designing the biomass pyrolysis industry [13]–[15]. Kinetic data in the form of reaction rate constants (k) and activation energy (E) of SPR pyrolysis with a Thermogravimetry Analyzer have been carried out by Jamilatun [12]. The results obtained are that the heating speed for the optimal plant design is 40 – 50°C/minute with Ea for the breakdown of proteins and carbohydrates ranging from 35.46 – 47.89 kJ/mol with the value of the reaction rate constant (k) at range (0.0168 – 0.1021) to (0.0995 – 0.4691) sec^{-1} [12], [16]. Pyrolysis kinetics data without and with a catalyst using a fixed bed reactor has also been carried out, with secondary cracking models with various amounts of catalyst used (10, 20, and 40 wt.%). The greater the amount of catalyst used, the smaller the Ea, optimally at 40 wt.%, namely the decomposition of SPR into char (3.00 kJ/mol) [7].

The data obtained using a Thermogravimetry Analyzer and a fixed-bed reactor to calculate the kinetics of the pyrolysis decomposition reaction have not been able to predict the movement of raw material oxygenate towards product components. Next, to estimate the motion of raw material oxygenate in dominant tar to aliphatic or aromatic products or coke + gas or product oxygenate. For this reason, it is necessary to simulate the calculation of the decomposition kinetics of the reaction, namely the reaction rate constant (k) and activation energy (E) of SPR pyrolysis using the 5-Lump model method. The data required is the weight percent of each component of the pyrolysis product obtained from the GC-MS tar and the weight data of coke + gas after the pyrolysis is complete.

1.1. Biomass Pyrolysis

Pyrolysis can be understood as a biomass process using hot media without oxygen. This is the first step in the combustion and gasification process [17]–[19]. The primary reaction for pyrolysis of biomass can be simplified in Fig.1.

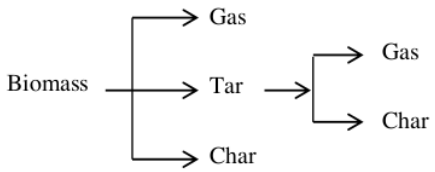

Fig. 1. Mechanism of pyrolysis reaction.

In general, the pyrolysis results are char in the form of solids and liquids (pyrolysis oil or tar) in a mixture of hydrocarbon compounds and gases [20]. According to Bridgwater [17], the residence time of the gas in the reactor, the pyrolysis temperature, and the heating rate are measured to classify the type of pyrolysis. Table 1 describes the variety of pyrolysis types.

Table 1. Types of biomass processes and yield composition [17]

Gas Residence Time	Temperature, °C	Process	Average composition (%)		
			Tar/Liquid	Char	Gas
> 1 hour	300–500	Carbonization	30	35	35
2–10 seconds	600–900	Gasification	5	10	85
0.1–2 seconds	400–650	Fast Pyrolysis	75	12	13

The mechanism of biomass decomposition is a complex process. Biomass pyrolysis occurs at 200°C to 400°C, often called a thermolysis event, the decomposition of compounds that make up biomass, such as cellulose, xylene, and pectin. The charcoal and aromatization process will be a second decomposition [21].

1.2. 5-Lump Kinetic Model

Pyrolysis of biomass involves many highly complex reactions and intermediate and final products. Therefore, modeling the kinetics of the pyrolysis reaction provides space for researchers to propose different reaction mechanisms. The biomass pyrolysis mechanism assumes biomass as the raw material, whereas gas/volatile, tar, and char as the main products [22]–[24].

The tar/bio-oil decomposition reaction is complex and produces thousands of compounds, so it is not easy to describe the kinetics of response at the molecular level. In the petroleum refining process, components are frequently grouped based on the similarity in boiling points and molecular characteristics [25]. This grouping model can determine the decomposition reaction kinetics model in tar upgrading with the 5-Lump model, as described in Fig.2.

The 5-Lump model is a model composed by grouping compounds into 5: the raw material oxygenate group (I) and

oxygenate product (III), aromatic product (II), aliphatic product (IV), and coke + gas product (V). In the decomposition process of oxygenate compounds of raw materials, catalytic cracking forms product oxygenates, aromatics, aliphatic compounds, and coke + gas.

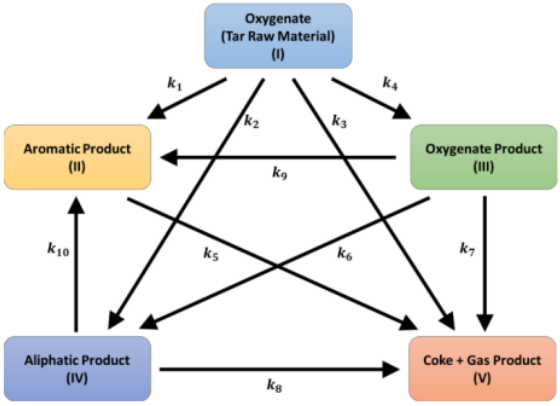

Fig. 2. The decomposition reaction of oxygenate compounds with the 5-Lump model.

One of the critical studies in reaction kinetics. Kinetic parameters are indispensable in process scale-up for industrial applications. El-Rub et al. [26] and Juneja et al. [27] conducted several kinetic studies following the first-order model that ignores the deactivation process. Cano et al. carried out the effect of catalyst deactivation in the kinetic model [28]. They stated that the conversion of tar in the gas during the process would decrease with increasing carbon deposits in the pores of the catalyst.

Some of the experimental conditions and assumptions used in the completion of the 5-Lump model are as follows:

1. The reactor consists of 2 cylinders arranged in series vertically; the top cylinder is filled with SPR (R1), and the bottom is filled with catalyst (R2) (Figure 5). The one-step process with batch system solid biomass feed on R1, and feed R2 is gas combustion product on pyrolysis in R1 (Ex-situ pyrolysis).
2. Heterogeneous reaction phase, solid silica-alumina catalyst in the gas phase.
3. The content of oxygenated compounds in the feed gas to R2 is similar to that of oxygenated compounds in the pyrolysis tar in R1. The content of tar feed that decomposed in the catalyst stack was supposed only to oxygenate compounds, while aliphatic and aromatic compounds were considered inert.
4. The amount of coke and gas formed out of R2 is assumed to be the amount of coke and gas passing through the catalyst stack at R2 minus the coke and gas produced at R1.
5. The weight fraction of the inlet oxygenate compound R2 is assumed to be = 1 = product oxygenate fraction + aromatic fraction + aliphatic fraction + coke and gas fraction.
6. The volume of gas flowing in the catalyst stack (V_Z) in R2 is the mass fraction of the oxygenate compound multiplied by the amount of combustion gas produced from uncatalyzed pyrolysis in R1.

The kinetic model developed by Dou [25] is formulated as a function of yield, deactivation, and reaction rate constant. The reaction rate equation based on Fig.2 for each group is:

a. Raw material oxygenate compound (C_I)

$$r_I = -(k_1 + k_2 + k_3 + k_4).C_I.a \quad (1)$$

b. Aromatic compounds (C_{II})

$$r_{II} = (k_1.C_I + k_9.C_{III} + k_{10}.C_{IV} - k_5.C_{III}).a \quad (2)$$

c. Product oxygenate compound (C_{III})

$$r_{III} = k_4.C_I.a - (k_6 + k_{7+}k_9).C_{III}.a \quad (3)$$

d. Aliphatic compound (C_{IV})

$$r_{IV} = (k_5.C_I + k_6.C_{III} - (k_8 + k_{10}).C_{IV}).a \quad (4)$$

e. Gas + coke (C_V)

$$r_V = (k_3.C_I + k_5.C_{II} + k_7.C_{III} + k_8.C_{IV}.a \quad (5)$$

The deactivation of the catalyst follows an exponential function $a = e^{-\alpha t}$.

In general, an increase in temperature will increase the reaction rate constant. The reaction rate constant and temperature relationship follow the Arrhenius equation [29], [30]. By experimenting with single-use catalysts concerning the research of El-Rub et al. [26] and Juneja et al. [27], the deactivation of the catalyst can be ignored and not included in the following calculation. From the derivation of the mathematical model of the pyrolysis reaction in a fixed-bed reactor and Equation (1) – (5), the Equation for the 5-Lump model can be written:

$$V_Z \frac{dC_I}{dZ} = -(k_1 + k_2 + k_3 + k_4).C_I.\rho_b.\varepsilon \quad (6)$$

$$V_z \frac{dC_{II}}{dz} = [k_1.C_I + k_9.C_{III} + k_{10}.C_{IV} - k_5.C_{III}].\rho_b.\varepsilon \quad (7)$$

$$V_z \frac{dC_{III}}{dz} = [k_4.C_I - (k_6 + k_{7+}k_9).C_{III}].\rho_b.\varepsilon \quad (8)$$

$$V_z \frac{dC_{IV}}{dz} = k_5.C_I + k_6.C_{III} - (k_8 + k_{10}).C_{IV}.\rho_b.\varepsilon \quad (9)$$

$$V_z \frac{dC_V}{dz} = [k_3.C_I + k_5.C_{II} + k_7.C_{III} + k_8.C_{IV}].\rho_b.\varepsilon \quad (10)$$

There are five (5) ordinary differential equations (Equations 6 – 10) and ten (10) algebraic equations (equations with i = 1, 2, 3, 4, 5, 6, 7, 8, 9, and 10) that can be solved simultaneously with numerical methods. The A_i and E_i are evaluated by trial and error until the simulated C_i value is close to the C_i value from the experimental data, more precisely, until the SSE value is minimal, as in Equation (11).

$$SSE = \sum(\langle C_i \rangle_{hitungan} - \langle C_i \rangle_{data})^2 \quad (11)$$

Figure 3 illustrates the flow of the solution to the 5-Lump ordinary differential equation.

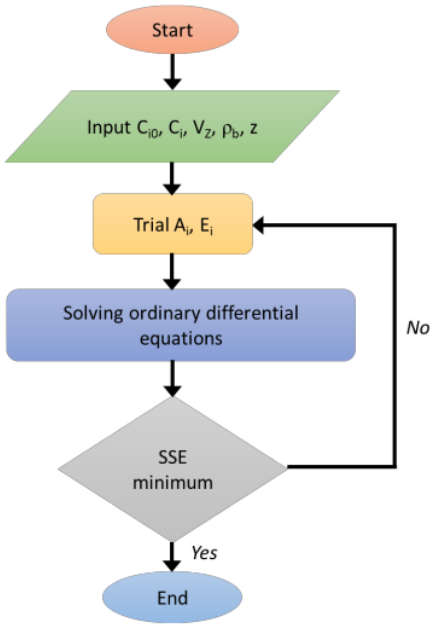

Fig. 3. The decomposition reaction of oxygenate compounds with the 5-Lump model.

2. Methodology

2.1. Materials

2.1.1. Spirulina platensis *residue (SPR)*

Nogotirto Algae Park provides Spirulina platensis (SP) microalgae. SP extraction produces algal oil and a solid *Spirulina platensis* residue (SPR). SPR analyzed calorific value, ultimate, and proximate. Proximate analysis (proteins using the Kjeldahl method; carbohydrates using the Anthrone method; lipids using the Soxhlet method) and calorific value (Bomb calorimeter) were carried out at the Laboratorium Pangan dan Hasil Pertanian, Departemen Teknologi Pertanian, Universitas Gadjah Mada dan Laboratorium Pangan dan Gizi PAU Universitas Gadjah Mada. While the ultimate (C, H, O, N, and S with the standard D2361) was carried out at the Laboratorium Penguji Puslitbang Tekmira Bandung [9], [12]. Sample test results are displayed in Table 2.

2.1.2. Alumina silica catalyst

PT Pertamina Balongan provides the need for silica-alumina catalysts still in the form of fine powder. Laboratorium Penelitian dan Pengujian Terpadu (LPPT) UGM conducted a BET (Brunaur, Emmett, and Teller) analysis in the form of (i) SiO_2/Al_2O_3 silica-alumina ratio, (ii) pore surface area, (iii) average pore volume/pore volume total, and SEM-EDX (Scanning Electron Microscope–Energy Dispersive X-ray) in the form of C, O, Al and Si content tests. The International Border Division, Department of Transdisciplinary Science and Technology of the School of Environment and Society, Tokyo Institute of Technology, Japan, conducted an XRF (X-ray Fluorescence) test [10], a composition test of SiO_2 and Al_2O_3. Table 3 presents the results of the catalyst test.

2.2. Equipment

SPR pyrolysis was carried out using a fixed-bed reactor. Experiments were carried out with and without a catalyst. Fixed-bed reactor made of stainless steel with reactor dimensions inside diameter (ID) = 4.0 cm, outside diameter (OD) = 4.4 cm, and height = 60.0 cm. The reactor consists of two horizontal cylinders equipped with electric heating through a nickel wire wound on the outer surface of the cylinder. The first cylinder is for SPR biomass (R1), and the second is for silica-alumina catalyst (R2). The pyrolysis gas product from R1 flows directly into R2, containing the stack of catalysts. Figure 4 presents a diagram of the reactor arrangement, while Figure 5 presents a fixed-bed reactor pyrolysis unit [10].

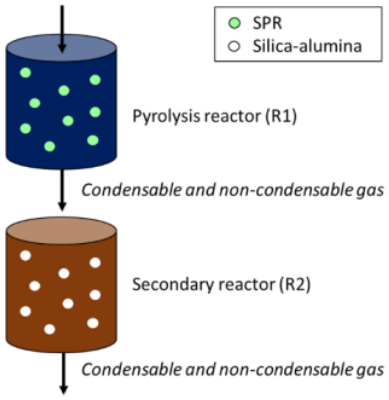

Fig. 4. Fixed-bed reactor arrangement.

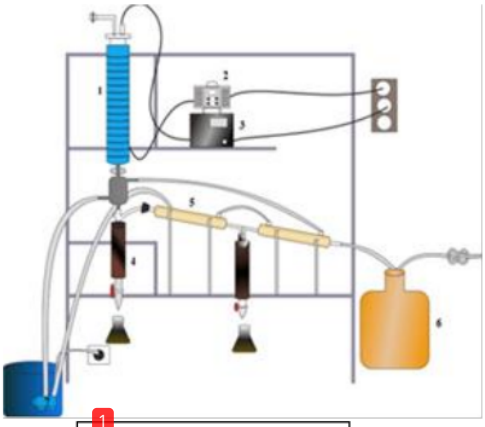

1. Reactor
2. Heater
3. Thermocouple
4. Accumulator of bio-oil
5. Condenser
6. Accumulator of gas
7. Pump

Fig. 5. Arrangement of experiment equipment.

2.3. Methods

2.3.1. Preparation of SPR and silica-alumina catalyst

The dried Spirulina platensis (SPR) residue was obtained from drying the wet SPR in the sun for three (3) days. The lumps of dirt were cleaned from the SPR and stirred so that the size distribution was homogeneous. Storage of SPR in a dry and closed container [9].

The silica-alumina catalyst in pellets is made by mixing 95% silica-alumina with 5% by weight of kaolin and added with sufficient aquadest. The mixture was stirred to make it homogeneous, then molded into pellets with a diameter of 0.4 cm and a height of 0.6 cm. The catalyst pellets were dried for three (3) days. To ensure dry pellets, they are heated in a furnace at a temperature of 500°C for 2 hours, then cooled in a desiccator [10].

2.3.2. *Pyrolysis*

Fifty (50) g SPR was added to reactor R1, while silica-alumina catalyst was added to R2 with a thickness variation of 1-4.5 cm. Next, the reactor was sealed and heated externally by an electric furnace, and a NiCr-Ni thermocouple was placed outside the furnace to control the temperature. The heating rate of the SPR pyrolysis is 5-35°C/min, heated from room temperature (30°C) to the desired temperature (300–600°C), then for 1 hour, the temperature is kept constant. The temperature rise is recorded every minute, and the heating rate is controlled—furthermore, the condensation of the pyrolysis gas. The condensed liquid product is collected in the accumulator, and the amount is measured. The liquid or tar product, a mixture of the oil phase (bio-oil) and the water phase, is separated by decantation. The yield of bio-oil, water phase, charcoal, and gas is calculated by Equation (12) – (15), while the conversion is calculated by Equation (16). After the experiment, the remaining amount of solid (char) was taken and weighed. The experiment was repeated three times for each tested variable. GC-MS analyzed tar products to determine the type and amount of compounds contained in tar. This data can be used to calculate the decomposition reaction kinetics of the 5-Lump model.

2.3.3. Variables of study

1) They are changing variables. For fixed-bed reactors, they include (i) temperature (300–600°C) and (ii) catalyst height in the reactor (0–4.5 cm) or catalyst weight (10, 20, 30, and 40 wt.%).

2) Fixed variables. For fixed-bed reactors, they include (i) heating rate (5–35°C/min), (ii) amount of SPR used (50 grams), (iii) type of catalyst (silica-alumina), and (iv) dimensions of silica catalyst alumina (pellet: 0.4 cm in diameter and 0.6 cm in height).

2.3.4. Analysis

1) Liquid Product. The liquid product in the form of tar was analyzed for its composition (oxygenate, aliphatic, aromatic, and nitrogenate) by GC-MS. GCMS devise with Shimadzu GCMS type [GCMS-QP2010 SE] Rastek Rxi-5MS column 30 m long, ID 0.25 mm with a Helium carrier gas, injector temperature 200°C, pressure 50.4 kPa, total flow 128 mL/minute, column flow 0.85 mL/minute. The analysis was carried out at the Research Laboratory, Faculty of Pharmacy, Universitas Ahmad Dahlan.

2) GC-MS data processing. Tar GC-MS data processing related to functional groups (oxygenate, aromatic, aliphatic, and nitrogenate) was carried out with: (i) oxygenates, all compounds containing O, (ii) aromatics, and all C and H compounds whose chains are in the form of rings, (iii) aliphatic, all compounds C and H with straight chains, and (iv) nitrogenates, all compounds containing N.

3. Results and Discussion

3.1. Spirulina platensis residue (SPR) and *Spirulina platensis* (SP)

The effect of extraction on the composition of *Spirulina platensis* (SP) and *Spirulina platensis* residue (SPR) raw materials was carried out through proximate, ultimate, and HHV analyses. Table 2 presents the results of the analysis.

Table 2. *Spirulina platensis* (SP) and *Spirulina platensis* residue (SPR) [12]

Component	SP	SPR
Analysis of composition (wt.%)		
Lipids	0.25	0.09
Carbohydrate	46.13	38.51
Protein	44.72	49.60
Analysis of proximate (wt.%)		
Moisture	11.83	9.99
Ash	8.63	8.93
Volatile	67.03	68.31
Fixed carbon	12.51	12.77
Analysis of ultimate (wt.%)		
Sulfur	0.49	0.55
Carbon	41.91	41.36
Hydrogen	6.82	6.60
Nitrogen	8.89	7.17
Oxygen	33.04	35.33
H/C, the molar ratio	1.95	1.91
O/C, the molar ratio	0.59	0.64
Higher heating value (MJ/kg)	20.09	18.21

From Table 2, it can be seen that SP and SPR have almost the same composition, such as ash (8.63−8.69 wt.%) and volatile (67.03−68.31 wt.%) and fixed carbon (12.51−12.77 wt.%). From the results of the ultimate analysis for components C (41.36−41.91 wt.%), H (6.60−6.82 wt.%), and N (7.17−8.89 wt.%). Except in O, there was a slight increase in SP, as much as 33.04 wt.%, and at SPR, 35.33 wt.%. Meanwhile, the lipids in SP (0.25 wt.%) and SPR (0.09 wt.%) were very low for proximate analysis. The conclusion from comparing the study results before and after extraction is that the material does not experience a significant change in composition. The lipid content in SP is shallow, so the extraction effect is not very visible [12].

3.2. *Characteristics of Silica Alumina Catalyst*

Silica alumina was analyzed using SEM-EDX. The results were in the form of elemental percentage and weight of the catalyst constituents, respectively as shown in Fig.6 and Table 3 below. Figure 6 explains the magnitude of the voltage (keV) used and the total counts of each catalyst constituent (C, O, Al and Si). For Si, the voltage obtained was 1.739 keV with 2,400 counts, while for Al was 1.486 keV with 6,800 counts.

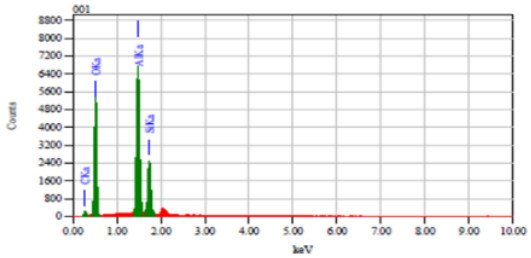

Fig. 6. Results of silica-alumina SEM-EDX analysis [10]

Based on the catalyst analysis with BET, SEM-EDX, and the composition in the form of SiO_2 and Al_2O_3 oxides with XRF analysis, the values can be seen in Table 3.

Table 3. Specifications of silica-alumina catalyst

	Si-Al specification	Value	
XRF	SiO_2	60.28 wt.%	
	Al_2O_3	35.25 wt.%	
	SiO_2/Al_2O_3	1.71	
BET	*Pore surface area*	240.553 m^2/g surface area	
	Pore diameter	3.3 nm	
	Average pore volume	0.199 cm^3/g total pore volume	
		Weight, wt.%	**Atoms, %**
SEM-EDX	C	8.41	12.74
	O	55.78	63.41
	Al	24.64	16.61
	Si	11.17	7.24

3.3. *Reaction Kinetics Test of 5-Lump Model*

This model consists of 5 groups, raw material oxygenate group (I), aromatic product (II), oxygenate product group (III), aliphatic product group (IV), and coke and gas product group (V). With this model, the reaction rate constant (k) of decomposition and the activation energy (E) of the oxygenate compound of the raw material into product components can be studied. To determine the relationship between the simulation results and the experimental data in each group (lump) at a temperature of 300 – 600°C at various thicknesses of the catalyst, see Figures 7 – 10.

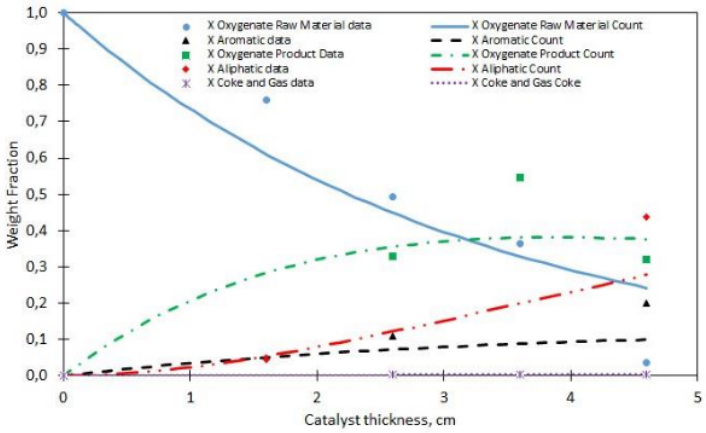

Fig. 7. The relationship between concentration and thickness of the catalyst bed (cm) at a temperature of 300°C with the 5-Lump model.

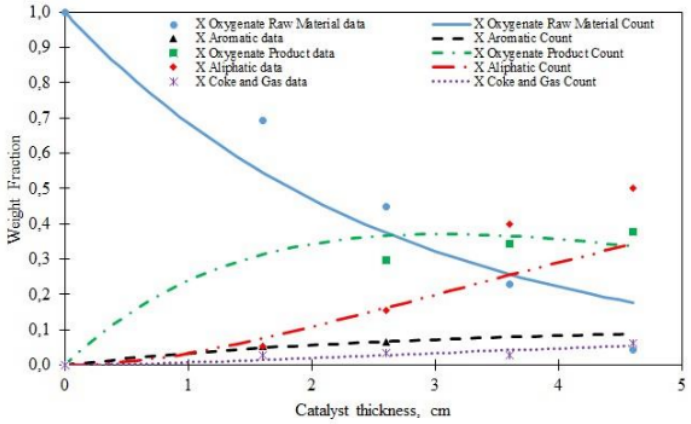

Fig. 8. The relationship between concentration and thickness of the catalyst bed (cm) at a temperature of 400°C with the 5-Lump model.

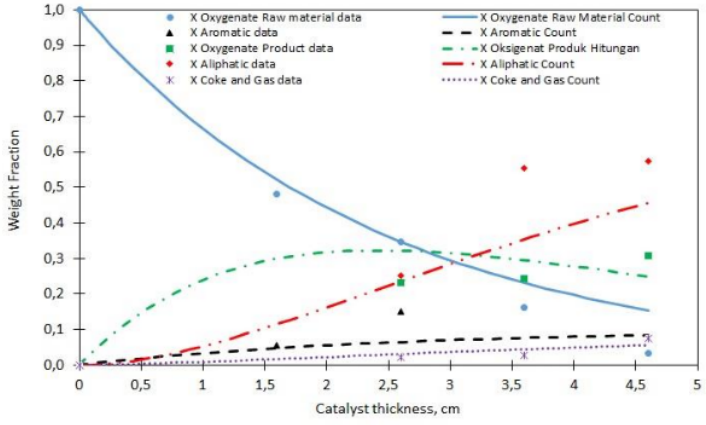

Fig. 9. The relationship between concentration and thickness of the catalyst bed (cm) at a temperature of 500°C with the 5-Lump model.

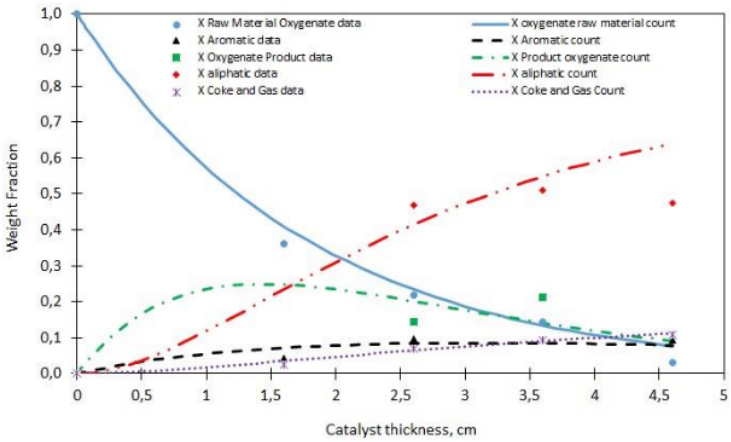

Fig. 10. The relationship between concentration and thickness of the catalyst bed (cm) at a temperature of 600°C with the 5-Lump model.

Based on Figures 7 – 10, it can be seen that the same trend at a temperature of 300 – 600°C is the effect of the thickness of the catalyst bed on the mass fraction of the product. The thicker the catalyst bed, the higher the mass fraction of the product. On the other hand, the oxygenate mass fraction of the raw material decreases sharply.

The raw material oxygenate compounds consist of anhydrosugars and furfurals produced through hydrolysis, cracking, and dehydration of carbohydrates. Oxygenate raw materials (anhydrosugars and furfurals) undergo decarboxylation and deoxygenation reactions to make the product of other oxygenates (ketones, aldehydes, acids, and alcohols), followed by cracking to form olefins. The oxygenate mass fraction of the product appears to be increasing very sharply. This indicates that with the thickness of the silica-alumina catalyst bed, decarboxylation and deoxygenation are dominant compared to cyclization, which will convert olefins into aromatics [31]. The results of the calculation of the value of the reaction rate constant from the 5-Lump model can be seen in Table 4.

Table 4. The value of the reaction rate constant for the catalytic kinetics of the components following the 5-Lump model

Reaction	Reaction rate constants, sec.$^{-1}$			
	300°C	400°C	500°C	600°C
k_1 (I → II)	2.466	2.760	3.298	4.044
k_2 (I → IV)	6.442	6.689	8.520	11.132
k_3 (I → V)	50.757	54.579	63.025	77.976
k_4 (I → III)	7.800	8.291	10.047	12.999
k_5 (II → V)	0.000	0.014	0.026	0.035
k_6 (III → IV)	11.779	11.823	11.830	11.835
k_7 (III → V)	0.000	0.004	0.008	0.010
k_8 (IV → V)	0.000	0.003	0.008	0.011
k_9 (III → II)	0.003	0.012	0.020	0.024
k_{10} (IV → II)	0.003	0.014	1.074	1.941
Correction, %	54.640	23.550	14.690	10.520

From the results of the calculation of the reaction rate constants in Table 4, it can be observed that at a temperature of 300 – 600°C, the reaction rate of the decomposition of oxygenate compounds of raw materials into coke and gas compounds (k_3) has the highest value (50.757–77.976 s.$^{-1}$), followed by k_6 (11.779–11.835 s.$^{-1}$), k_4 (7.8–12.999 s.$^{-1}$), k_2 (6.442–11.132 s.$^{-1}$) and k_1 (2.446–4.044 s.$^{-1}$). In contrast, the value for another k (k_5, k_7, k_8, k_9, k_{10}) is minimal. This phenomenon shows that breaking C–O and H–O bonds from oxygenating compounds is more accessible than breaking C–H and C–C bonds from aromatic, aliphatic, and coke and gas. The rate constant for the decomposition reaction (k_3) of oxygenate compounds (I) into coke and gas (V) has the highest value compared to the other k. This tendency shows that oxygenate compounds undergo C–O and H–O termination more efficiently and produce CO, CO_2, and other gases. With increasing temperature, the yield of gas produced is higher. Sunarno et al. (2017) have investigated the reaction kinetics of the lumped method of catalytic cracking of bio-oil produced from the pyrolysis of empty oil palm bunches; the result is that the reaction rate constant increases with increasing temperature [32].

Meanwhile, the value of the collision frequency factor (A) and the activation energy (E) of the 5-Lump model using the Arrhenius equation can be seen in Table 5.

Table 5. Value of collision frequency factor (A) and activation energy (E) with 5-Lump model

Reaction	A	E (kJ/mol)
k_1 (I → II)	9.72	6.73
k_2 (I → IV)	28.57	7.47
k_3 (I → V)	161.26	5.73
k_4 (I → III)	30.88	6.86

k_5 (II → V)	1,956.97	73.78
k_6 (III → IV)	11.95	0.07
k_7 (III → V)	20.55	52.11
k_8 (IV → V)	33.43	55.34
k_9 (III → II)	2.43	31.66
k_{10} (IV → II)	2.77x10^6	101.05

From Table 5, it can be seen that the most negligible activation energy (0.07 kJ/mol) occurs in the k_6 reaction (III-IV), namely, the product oxygenate (III) becomes aliphatic (IV). The following is the order of activation energy starting from the smallest value, namely k_6 (III-IV) (0.07 kJ/mol); k_3 (I → V) (5.73 kJ/mol); k_1 (I → II) (6.73 kJ/mol); k_4 (I → III) (6.86 kJ/mol); k_2 (I → IV) (7.47 kJ/mol); k_9 (III-II) (31.66 kJ/mol); k_7 (III → V) (52.11 kJ/mol); k_8 (IV → V) (55.34 kJ/mol); k_5 (II → V) (73.78 kJ/mol) and k_{10} (IV-II) (101.05 kJ/mol). The value of E indicates that oxygenate compounds are more accessible to decompose than aromatic and aliphatic compounds.

Based on Table 5, the reaction with the highest activation energy (101.05 kJ/mol) shows the most challenging reaction occurring, which is aliphatic (IV) to aromatic (II). The order of activation energy values from the largest is 73.78 kJ/mol, which is aromatic (II) to coke and gas (V), followed by 55.34 kJ/mol, which is aliphatic (IV) to coke and gas (V); 52.11 kJ/mol which is product oxygenate (III) into coke and gas (V); and 31.66 kJ/mol which is from product oxygenate (III) to aromatic (II). Decomposition reaction from product oxygenate (III) into aliphatic (IV) was more accessible than into aromatic (II) or coke and gas (V). The tendency of aliphatic formation of oxygenate compounds is very relevant to the study of slow pyrolysis of SPR, where the higher the pyrolysis temperature, the higher the aliphatic compounds [33].

4. Conclusion

This paper aims to review the kinetics of the pyrolysis catalytic decomposition reaction using the 5-Lump kinetic model. From the calculation results at a temperature of 300-600°C, the optimum activation energy is obtained at the reaction rate constant, k_6 (11,779 – 11,835 s^{-1}) with E_6 = 0.07 kJ/mol and the reaction rate constant, k_3 (50,757 – 77,976 s^{-1}) with E_3 = 5.73 kJ/mol. The lowest activation energy in the reaction of oxygenate compounds (III) decomposes to form aliphatic compounds (IV) indicating that the reaction is the easiest to occur. Oxygenate compounds are more easily cut at the C–O and H–O bonds, producing CO, CO_2, and aliphatic compounds. The highest value of E is at k_{10}, namely the formation of aromatics (II) from aliphatic compounds (IV) with E_{10} = 101.05 kJ/mol. A large E value indicates the difficulty of decomposing aliphatic compounds into aromatics. The thicker the catalyst used in the fixed-bed reactor, the higher the product mass fraction in the form of product oxygenate, aliphatic, aromatic, coke, and gas compounds. On the other hand, the oxygenate compound in the pyrolysis feed decreased sharply.

Acknowledgments

The author would like to thank all who have helped complete the review of this article, either directly or indirectly.

NOTATION LIST

Notation		Definition
r_I	:	Rate of decomposition of oxygenate compounds
r_{II}	:	Rate of reaction for the formation of aromatic product compounds
r_{III}	:	Rate of reaction for the formation of oxygenating product
r_{IV}	:	Rate of reaction for the formation of aliphatic product
r_{RV}	:	Rate of reaction for the formation of coke + gas product
k_1	:	The reaction rate constant for the decomposition of oxygenate compounds into aromatic products, (s^{-1})
k_2	:	The reaction rate constant for the decomposition of oxygenate compounds into aliphatic products, (s^{-1})
k_3	:	The reaction rate constant for the decomposition of oxygenate compounds into coke compounds + gas product, (s^{-1})
k_4	:	The reaction rate constant for the decomposition of oxygenate compounds into oxygenating products, (s^{-1})
k_5	:	The reaction rate constant for the decomposition of aromatic product compounds into coke + gas products, (s^{-1})
k_6	:	The reaction rate constant for the decomposition of oxygenating product compounds into aliphatic product compounds, (s^{-1})
k_7	:	The reaction rate constant for the decomposition of oxygenating product compounds into coke compounds + gas product, (s^{-1})
k_8	:	The reaction rate constant for the decomposition of aliphatic product compounds into coke compounds + gas products, (s^{-1})
k_9	:	The reaction rate constant for the decomposition of oxygenating product compounds into aromatic products, (s^{-1})
k_{10}	:	The reaction rate constant for the decomposition of aliphatic product compounds into aromatic products, (s^{-1})
C_i	:	The concentration of oxygenated compounds (mol/com^3)
C_{II}	:	The concentration of aromatic product compounds (mol/com^3)
C_{III}	:	The concentration of oxygenating product compound (mol/com^3)
C_{IV}	:	The concentration of aliphatic product compound (mol/com^3)
C_v	:	The concentration of compounds coke + gas product (mol/com^3)
a	:	Catalyst deactivation
ϵ	:	The reaction activation energy (J/mol)
V_z	:	Steam superficial velocity (cm^3/cm^2.minute)
ρ_b	:	The specific gravity of the flowing gas, gr/cm^3
ε	:	Free space fraction of catalyst stack

References

[1] G. Kumar, S. Shobana, W. Chen, Q. Bach, S. H. Kim, A. E. Atabani, J. S. Chang, "A review of thermochemical conversion of microalgal biomass for biofuels: chemistry and processes," *Green Chemistry*, vol. 19, pp. 44–67, 2017, doi: 10.1039/C6GC01937D.

[2] A. Aho, N. DeMartini, A. Pranovich, J. Krogell, N. Kumar, K. Eränen, B. Holmbom, T. Salmi, M. Hupa, D. Yu. Murzin, "Pyrolysis of pine and gasification of pine chars – Influence of organically bound metals," *Bioresource Technology*, vol. 128, pp. 22–29, 2013, doi: 10.1016/j.biortech.2012.10.093.

[3] Y. L. Tan, A. Z. Abdullah, and B. H. Hameed, "Product distribution of the thermal and catalytic fast pyrolysis of Karanja (Pongamia pinnata) fruit hulls over a reusable silica-alumina catalyst," *Fuel*, vol. 245, pp. 89–95, 2019, doi: 10.1016/j.fuel.2019.02.028.

[4] S. P. Jeevan Kumar, V. K. Garlapati, A. Dash, P. Scholz, and R. Banerjee, "Sustainable green solvents and techniques for lipid extraction from microalgae: A review," *Algal Research*, vol. 21, pp. 138–147, 2017, doi: 10.1016/j.algal.2016.11.014.

[5] T. Kan, V. Strezov, and T. J. Evans, "Lignocellulosic biomass pyrolysis: A review of product properties and effects of pyrolysis parameters," *Renewable and Sustainable Energy Reviews*, vol. 57, pp. 1126–1140, 2016, doi: 10.1016/j.rser.2015.12.185.

[6] G. Kabir and B. H. Hameed, "Recent progress on catalytic pyrolysis of lignocellulosic biomass to high-grade bio-oil and bio-chemicals," *Renewable and Sustainable Energy Reviews*, vol. 70, pp. 945–967, 2017, doi: 10.1016/j.rser.2016.12.001.

[7] A. Hassan, S. Zafar Ilyas, H. Mufti, "Review of the renewable energy status and prospects in Pakistan" *International Journal of Smart Grid - ijSmartGrid*, vol. 5,no.4,2021,doi:doi.org/10.20508/ijsmartgrid.v5i4.220.g174.

[8] K. Okedu, M. Al-Hashmi, "Assessment of the Cost of various Renewable Energy Systems to Provide Power for a Small Community: Case of Bukha, Oman," *International Journal of Smart Grid - ijSmartGrid*, vol. 2,no.3,2018,doi:doi.org/10.20508/ijsmartgrid.v2i3.17.g179.

[9] A. Harrouz, A. Temmam, M. Abbes, "Renewable Energy in Algeria and Energy Management Systems," *International Journal of Smart Grid - ijSmartGrid*, vol.2,no.1,2018,doi:doi.org/10.20508/ijsmartgrid.v2i1.10.g9.

[10] S. Jamilatun, A. Budiman, H. Anggorowati, A. Yuliestyan, Y. Surya Pradana, and Budhijanto, "Ex-Situ Catalytic Upgrading of Spirulina platensis residue Oil Using Silica Alumina Catalyst," *International Journal of Renewable Energy Research*, vol. 9, no. 4, 2019, doi: 10.20508/ijrer.v9i4.10119.g7776.

[11] S. Jafarian and A. Tavasoli, "A comparative study on the quality of bioproducts derived from catalytic pyrolysis of green microalgae Spirulina (Arthrospira) plantensis over transition metals supported on HMS-ZSM5 composite," *International Journal of Hydrogen Energy*, vol. 43, pp. 1–16, 2018, doi: 10.1016/j.ijhydene.2018.08.171.

[12] B. Qiua, X. Tao, J. Wang, Y. Liu, S. Li, H. Chu, "Research progress in the preparation of high-quality liquid fuels and chemicals by catalytic pyrolysis of biomass: A review," *Energy Conversion and Management*,vol.261,2022,doi:doi.org/10.1016/j.enconman.2022.115647.

[13] S. J. Ojolo, C. A. Oshekub, and M. G. Sobamowoa, "Analytical investigations of kinetic and heat transfer in slow pyrolysis of a biomass particle," *International Journal of Renewable Energy Development*, vol. 2, no. 2, pp. 105–115, 2013, doi: 10.14710/ijred.2.2.105-115.

[14] H. Shafaghat, P. S. Rezaei, D. Ro, J. Jae, B. S. Kim, S. C. Jung, B. H. Sung, Y. K. Park, "In-situ catalytic pyrolysis of lignin in a bench-scale fixed bed pyrolyzer," *Journal of Industrial and Engineering Chemistry*, vol. 54, pp. 447–453, 2017, doi: 10.1016/j.jiec.2017.06.026.

[15] M. Hu, Z. Chen, D. Guo, C. Liu, B. Xiao, Z. Hu, S. Liu, "Thermogravimetric study on pyrolysis kinetics of Chlorella pyrenoidosa and bloom-forming cyanobacteria," *Bioresource Technology*, vol. 177, pp. 41–50, 2015, doi: 10.1016/j.biortech.2014.11.061.

[16] A.P.S. Dias, B. Rijo, M. Ramos, M. Casquilho, A. Rodrigues, H. Viana, F. Rosaa,"Pyrolysis of burnt maritime pine biomass from forest fires," *Biomass and Bioenergy*, vol. 163, 2022, doi:doi.org/10.1016/j.biombioe.2022.106535.

[17] A. V Bridgwater, "Renewable Fuels and Chemicals by Thermal Processing of Biomass," *Chemical Engineering Journal*, vol. 91, no. 2–3, pp. 87–102, 2003, doi: 10.1016/S1385-8947(02)00142-0.

[18] Y. L. Tan, A. Z. Abdullah, and B. H. Hameed, "Catalytic fast pyrolysis of durian rind using silica-alumina catalyst: Effects of pyrolysis parameters," *Bioresource Technology*, vol. 264, pp. 198–205, 2018, doi: 10.1016/j.biortech.2018.05.058.

[19] S. Wang, G. Dai, H. Yang, and Z. Luo, "Lignocellulosic biomass pyrolysis mechanism: A state-of-the-art review," *Progress in Energy and Combustion Science*, vol. 62, pp. 33–86, 2017, doi: 10.1016/j.pecs.2017.05.004.

[20] V. Anand, V. Sunjeev, and R. Vinu, "Catalytic fast pyrolysis of Arthrospira platensis (spirulina) algae using Zeolites," *Journal of Analytical and Applied Pyrolysis*, vol. 118, pp. 298–307, 2016, doi: 10.1016/j.jaap.2016.02.013.

[21] T. Fisher, M. Hajaligol, B. Waymack, and D. Kellog, "Pyrolysis Behaviour and Kinetics of Biomass Derived Materials," *Journal of Analytical and Applied Pyrolysis*, vol. 62, no. 2, pp. 331–349, 2002, doi:

10.1016/S0165-2370(01)00129-2.

[22] A. Anca-Couce, "Reaction mechanisms and multi-scale modeling of lignocellulosic biomass pyrolysis," *Progress in Energy and Combustion Science*, vol. 53, pp. 41–79, 2016, doi: 10.1016/j.pecs.2015.10.002.

[23] N. Prakash and T. Karunanithi, "Kinetic modeling in biomass pyrolysis – A Review," *Journal of Applied Sciences Research*, vol. 4, no. 12, pp. 1627–1636, 2008.

[24] Q.-V. Bach and W. . Chen, "Pyrolysis characteristics and kinetics of microalgae via thermogravimetric analysis (TGA): A state-of-the-art review," *Bioresource Technology*, vol. 246, pp. 88–100, 2017, doi: 10.1016/j.biortech.2017.06.087.

[25] B. Dou, W. Pan, J. Ren, B. Chen, J. Hwang, and T. Yu, "Removal of tar component over cracking catalysts from high temperature fuel gas," *Energy Conversion and Management*, vol. 49, no. 8, pp. 2247–2253, 2008, doi: 10.1016/j.enconman.2008.01.027.

[26] Z. A. El-Rub, E. A. Bramer, and G. Brem, "Experimental comparison of biomass chars with other catalyst for tar reduction," *Fuel*, vol. 87, no. 10–11, pp. 2243–2252, 2008, doi: 10.1016/j.fuel.2008.01.004.

[27] A. Juneja, S. Mani, and J. Kastner, "Catalytic cracking of tar using biochar as a catalyst," in *2010 ASABE Annual International Meeting*, 2010, p. 13, doi: 10.13031/2013.30003.

[28] D. F. Cano, A. G. Barea, S. Nilssson, and P. Ollero, "Decomposition kinetics of model tar compounds over chars with different internal structure to model hot tar removal in biomass gasification," *Chemical Engineering Journal*, vol. 228, pp. 1223–1233, 2013, doi: 10.1016/j.cej.2013.03.130.

[29] H. S. Fogler, *Element of Chemical Reaction Engineering*, 3rd ed. Prentice-Hall International, Inc, 2006.

[30] O. Levenspiel, *Chemical Reaction Engineering*, 3rd ed. New York: John Wiley & Sons, Inc, 1999.

[31] C. Yang, R. Li, B. Zhang, Q. Qiu, B. Wang, H. Yang, Y. Ding, C. Wang, "Pyrolysis of microalgae: A critical review," *Fuel Processing Technology*, vol. 186, pp. 53–72, 2019, doi: 10.1016/j.fuproc.2018.12.012.

[32] Sunarno, Rochmadi, P. Mulyono, M. Aziz, and A. Budiman, "Kinetic Study of Catalytic Cracking of Bio-oil over Silica- alumina Catalyst," *BioResources*, vol. 13 (1), pp. 1917-1929, 2018.

[33] H. Siddiqi, A. Mishra, P. Maiti, I. D. Behera, B.C. Meika, "In-situ and ex-situ co-pyrolysis studies of waste biomass with spent motor oil: Elucidating the role of physical inhibition and mixing ratio to enhance fuel quality," *Bioresource Technology*, vol. 358, 2022, doi: doi.org/10.1016/j.biortech.2022.127364

Artikel 18

ORIGINALITY REPORT

8%	8%	6%	0%
SIMILARITY INDEX	INTERNET SOURCES	PUBLICATIONS	STUDENT PAPERS

PRIMARY SOURCES

1	journal.ugm.ac.id Internet Source	3%
2	www.ijrer.com Internet Source	2%
3	ijrer.org Internet Source	2%

Exclude quotes	On	Exclude matches	< 2%
Exclude bibliography	Off		